

Chemical Reactivity of Uranium Trioxide

Part 1.—Conversion to U_3O_8 , UO_2 and UF_4

BY R. M. DELL AND V. J. WHEELER

Chemistry Division, A.E.R.E., Harwell, Berks.

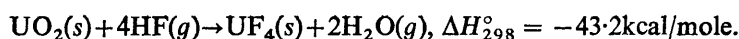
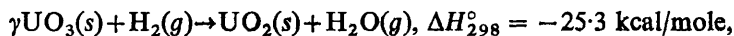
Received 26th January, 1962

A kinetic study has been made of the reduction of UO_3 to UO_2 by hydrogen and carbon monoxide and of the conversion of UO_2 to UF_4 by hydrogen fluoride. The reduction reaction is an interfacial reaction proceeding via the $UO_{2.6}$ phase, with CO reacting more readily than H_2 . The reactivity of UO_2 towards HF is a function of its surface area which increases with (a) lower reduction temperature, (b) the presence of sulphate impurity in the UO_3 .

The decomposition of UO_3 to U_3O_8 and conversion of the latter to UO_2 and UF_4 has been studied also and the kinetics are reported. The rate of hydrofluorination of UO_2 prepared by this route is dependent upon the UO_3 decomposition temperature rather than upon the U_3O_8 reduction temperature. It is shown that for UO_2 to be reactive towards HF it must possess both an adequate surface area ($> 2m^2/g$) and sufficient internal porosity to accommodate the volume increase associated with conversion to UF_4 .

Some experiments on the interaction of UO_2 single crystals with HF are reported also.

Uranium trioxide is known to form five different crystallographic phases (designated α - ϵ) and an amorphous phase.¹ The reduction of UO_3 to UO_2 by hydrogen and its subsequent conversion to UF_4 by reaction with hydrogen fluoride are processes which have been studied extensively in the atomic energy industry, using principally γUO_3 prepared from uranyl nitrate hexahydrate and βUO_3 prepared from ammonium diuranate. Both reactions are exothermic, viz.,



A review of unpublished work has been compiled by Harrington and Ruehle.² The reactivity of UO_2 towards "hydrofluorination" depends upon its physical properties (particle size, porosity, surface area, etc.) which, in turn, are governed by the kinetics of the reduction reaction and by the origin and structure of the UO_3 . UO_2 of widely differing reactivity may be prepared.

The hydrogen reduction of UO_3 has been investigated recently by De Marco and Mendel³ using high surface area ($26 m^2/g$) amorphous UO_3 and by Notz and Mendel⁴ using γUO_3 of surface area $3 m^2/g$. Reduction was found to take place in two distinct steps propagating sequentially, viz., $UO_3 \rightarrow UO_{2.6}$ and $UO_{2.6} \rightarrow UO_2$. The intermediate $UO_{2.6}$ phase is stable over a range of composition from $UO_{2.65}$ to $UO_{2.56}$ and loses oxygen progressively until, at the composition $UO_{2.56}$, UO_2 nucleates. Using high surface-area oxide, which can be reduced at low temperatures, it is possible to separate the two reactions completely; with low surface-area UO_3 both reactions take place concurrently, the second reduction step lagging behind the first.

Recently, interest has arisen in a type of γUO_3 with an unusual and characteristic particle texture prepared by spray denitration of $UO_2(NO_3)_2 \cdot 6H_2O$ in a fluidized-bed reactor.⁵ The reduction of this material to UO_2 , followed by conversion to UF_4 , has been investigated by Tomlinson and coworkers.^{6,7} The present research

comprises an independent study of the reactivity of this type of UO_3 . Many of Tomlinson's results have been confirmed and in this paper we report an extension of the investigation to include (i) the decomposition of UO_3 to U_3O_8 and its subsequent reduction to UO_2 and conversion to UF_4 ; (ii) the reduction of UO_3 by CO ; (iii) the dependence of reactivity upon particle texture; (iv) the reaction of single crystals of UO_2 with HF .

The interest in the conversion of UO_3 to UF_4 stems principally from the importance of UF_4 as an intermediary, which may be either reduced directly to uranium metal or fluorinated to UF_6 for use in isotopic enrichment by gaseous diffusion. However, this study of the preparation of UF_4 has led to several observations which are believed to be of wider interest and application in the field of solid-gas reactions generally. It is these general features that we wish to emphasize in the present and succeeding papers.

EXPERIMENTAL

Reaction kinetics were measured with a thermobalance comprising a thermostatted copper-beryllium helical spring from which was suspended, by means of a 0.001 in. diam. platinum wire, a small platinum bucket (capacity 0.03 ml) containing approximately 70 mg of UO_3 . Changes in weight were measured by observing the movement of the support wire with a cathetometer. The use of small experimental samples minimized heat dissipation and gas diffusion problems. The bucket was provided with a loose-fitting cover, to prevent loss of solid by decrepitation; care was taken, however, to ensure free access of gas to the sample. Springs of sensitivity ~ 1 mm/mg were employed and measurements were made to an accuracy of ± 0.03 mm. The sample bucket was suspended freely in a platinum reaction tube which was supported rigidly in a vertical tube furnace. Electrically heated, all-nickel plumbing was used for the gas supply which was introduced to the base of the furnace. A steady flow of nitrogen ("oxygen-free") passed down over the spiral spring; this mixed at the top of the furnace with an upward flow of reactant gas and the mixed gases then passed through a side arm to disposal. The downward current of nitrogen served to eliminate corrosion by HF , as well as oscillations of the spring which are often observed when rising convection currents are present. This dynamically balanced system gave very satisfactory results once the influence of the flowing gases on the rest position of the spring had been established and calibrated. The rest position remained quite steady for given flow-rates, there being no observable drift or oscillation. The characteristics of this system have been described elsewhere.⁸ Hydrogen fluoride was metered from a thermostatted cylinder at a rate of 3.7 l./h using an orifice flowmeter. This flow-rate, if completely utilized, would be adequate to convert a 70 mg sample to UF_4 in 20 sec. The reaction rate was shown to be independent of flow-rate over a two-fold range. High purity cylinder hydrogen was passed through a Baker Deoxy converter and dried over magnesium perchlorate and by a trap at -195°C . Carbon monoxide was passed over heated copper to decompose any iron carbonyl present and dried similarly. No evidence was found for the formation of nickel carbonyl under the conditions employed. The flow-rate used was 0.9 l./min for H_2 and 0.6 l./min for CO .

The reaction temperature was controlled by a potentiometric controller and measured by a Pt/Pt—Rh thermocouple welded to the outside of the Pt reaction tube opposite the suspended sample. Calibrations were made frequently of the constant temperature zone in the tube and also of the temperature drop across the reactor wall for temperatures from 200° to 700°C . At 500°C this correction, which was independent of the gas flow-rates used, was 15°C . The corrected temperature was accurate to $\pm 2^\circ\text{C}$.

In a typical run the sample was heated to temperature at a constant rate (18 deg./min) in a stream of nitrogen. The decomposition of UO_3 to U_3O_8 was studied in nitrogen but for other reactions the appropriate gas was introduced when the desired steady temperature had been attained. Hydrofluorination experiments were always carried out immediately after the reduction of UO_3 to UO_2 . The necessary temperature adjustment between runs was made while hydrogen was still flowing. Care was taken to ensure that the reaction rate was not

limited by gas diffusion through the oxide bed; check experiments with samples differing in mass by a factor of two gave identical results, while unloading and examination layer by layer of a sample of partially reduced UO_3 showed no evidence for non-uniform reaction through the solid bed.

Physical measurements were made on samples of material sieved to 80-120 B.S.S. mesh size (particle diam. 130-200 microns). Surface areas were computed by the B.E.T. method from krypton adsorption isotherms at -195°C . A value of 19.4 \AA^2 was taken for the cross-sectional area of an adsorbed krypton atom. Pore-size distributions were measured directly with a mercury porosimeter and also computed from nitrogen adsorption isotherms.

Solid densities were determined by (a) carbon tetrachloride displacement (using Archimedes immersion method), and (b) mercury displacement (using a pycnometer). In each case the solid was first outgassed thoroughly at room temperature. Carbon tetrachloride, also outgassed, enters the open pores of the solid; this density value may, therefore, be used, in conjunction with the X-ray crystallite density, to determine the closed porosity of the particles. Mercury, however, is non-penetrating at 1 atm and may be used to calculate the total porosity. X-ray powder diffraction patterns were taken using a Guinier micro-focus camera. Photomicrographs of particle cross-sections were obtained by mounting the specimens in resin, followed by abrading and polishing.

MATERIALS

"Fluidized-bed" UO_3 was prepared by the spray denitration of high-purity uranyl nitrate solution at 300°C .⁶ It is well known in the industry that the surface area and reactivity of UO_2 prepared from uranyl nitrate (via UO_3) is significantly enhanced by the addition of $\sim 0.1\%$ of sulphuric acid to the uranyl nitrate solution. No completely satisfactory explanation of this fact has been advanced. In the present work we have employed both "low sulphate" UO_3 (of residual sulphate content 90 p.p.m.) and "sulphated" UO_3 (sulphate content standardized at 1000 p.p.m.). The only other impurity of significance was $\sim 0.4\%$ residual nitrate in each sample which was lost on heating to 500°C . The reactivity experiments using low sulphate UO_3 were all carried out with samples taken from a single large preparation which was unsieved. In the work with sulphated UO_3 , where we were interested in the influence of particle texture on reactivity, samples were taken from ten separate UO_3 preparations (denoted $\text{UO}_3\text{I-UO}_3\text{X}$) made in spray denitrator reactors of varying capacity over a period of two years. These samples varied significantly in colour (yellow-orange), appearance and texture. In order to discriminate against variations in reactivity arising from variations in particle size distribution, these preparations were all sieved, the 80-120 mesh fraction being accepted.

UO_2 crystals were prepared by fused salt electrolysis of uranyl chloride dissolved in an alkali halide eutectic melt.⁹

RESULTS

STRUCTURE OF FLUIDIZED-BED UO_3 PARTICLES

Microscopic examination of fluidized-bed UO_3 particles reveals a characteristic internal structure. The particles are roughly spherical and most consist of a central core of oxide surrounded by a hard, non-porous, outer shell of noticeably different appearance. Some particles possess a concentric layer ("onion-ring") type structure, built up by successive depositions of UO_3 , while still others consist of an assembly of primary spherical particles "cemented" together by further trioxide. X-ray examination revealed γUO_3 as the only phase detectable. Plate 1 shows the particle cross-sections of a typical sample in which the "core and shell" type particle predominates. In plate 2 an onion-ring type particle has been sectioned and a "core and shell" particle is shown with the shell partly broken away and inverted. The formation of particles with these characteristic textures may be understood in terms of the mode of operation of a fluidized-bed spray denitrator. In particular, experiments suggest

that the particle shells arise through sintering of the primary solid in the steam + nitric acid atmosphere of the reactor. Particle aggregates result from malfunctioning of the spray gun. For the present paper, however, we are concerned not with the detailed mechanism of particle formation, but rather with the influence of particle texture upon reactivity.

The surface area of low sulphate UO_3 was found to be a function of out-gassing temperature, ranging from $0.07 \text{ m}^2/\text{g}$ for a sample outgassed at 20°C to $0.15 \text{ m}^2/\text{g}$ for a sample outgassed at 400°C . This increase is a consequence of the loss of residual nitrate. To obtain corresponding data on the surface area of material within the particle cores, large particles were mildly crushed and fragments of a comparable size range (80-120 mesh) selected. The surface area of these, after outgassing at 20°C and 400°C , was $0.18 \text{ m}^2/\text{g}$ and $0.35 \text{ m}^2/\text{g}$ respectively. It is concluded that the cores of the particles are more porous than the shells, though by no means rich in pores of small dimensions. Rather, it seems likely that the core is formed from relatively loosely packed, essentially non-porous, crystallites. The CCl_4 density of uncrushed low sulphate UO_3 was almost independent of particle size, ranging from 7.10 g/cm^3 to 7.14 g/cm^3 with mercury densities being about 2 % lower. This small difference may arise from factors inherent in the different measuring techniques using carbon tetrachloride and mercury. In any event, it is clear that few micropores intersect the surface, a conclusion in agreement with mercury porosimeter measurements which indicate the absence of open pores of dimensions $> 100 \text{ \AA}$. The internal closed porosity is difficult to assess as the X-ray density of γUO_3 is not known with certainty. A reasonable value is $7.3\text{-}8.0 \text{ g/cm}^3$, leading to a closed porosity for these particles of 3-12 %.

REDUCTION OF UO_3 BY HYDROGEN

A detailed study was made of the kinetics of reduction of the standard sample of unsulphated UO_3 . The kinetic curves are shown in fig. 1. These curves possess the sigmoidal shape characteristically observed with fluidized-bed UO_3 .⁶ Examination of partially reduced particles reveals an outer shell of black UO_2 containing a central orange region of unconverted UO_3 (plate 3). This confirms that reaction proceeds through the particle by a phase-boundary mechanism. The kinetics were analyzed according to the "decreasing sphere" model using the Spencer-Topley equation $1 - (1 - c)^{\frac{1}{3}} = kt/r_0$ (where c = fraction converted at time t , r_0 = initial particle radius).¹⁰ Linear plots were obtained over the second half of the reaction (fig. 2) and from their slopes an activation energy of $28 \pm 2 \text{ kcal/mole}$ was calculated. This use of the Spencer-Topley equation, applied to an assembly of particles of varying size and reactivity, is recognized to be an over-simplification; however, empirically it gives linear plots and is considered to be a closer approximation to the truth than a first-order law which takes no account of the observed interfacial nature of the reaction.⁶ X-ray study of partially reduced samples, after quenching to room temperature and crushing, revealed the presence of three phases (UO_3 , $\text{UO}_{2.6}$, UO_2), thereby confirming that reduction proceeded by way of the non-stoichiometric $\text{UO}_{2.6}$ phase as an intermediary. In order to determine whether the sigmoidal shape of the reduction curves resulted from the summation of the two separate reaction steps or was a consequence of the physical structure of the particles, some experiments were carried out on the reduction of *crushed* samples of UO_3 . The curves were found to be linear up to the start of the decay period (70 % conversion) for several different reduction temperatures. It is concluded that the sigmoidal reduction curves are a consequence of the UO_3 particle structure, the shells of the particles reducing more slowly than the cores.

Measurements were made also of the change in surface area and particle density during the reduction of low-sulphate UO_3 to UO_2 . The results are summarized in table 1, along with other data appropriate to later sections. The surface area increased during reduction from $\sim 0.1 \text{ m}^2/\text{g}$ for UO_3 to $1.2 \text{ m}^2/\text{g}$ for UO_2 . With increasing reduction temperature from 520°C to 620°C the surface area of the product UO_2 decreased from $1.8 \text{ m}^2/\text{g}$ to $1.2 \text{ m}^2/\text{g}$. It should be noted that these surface

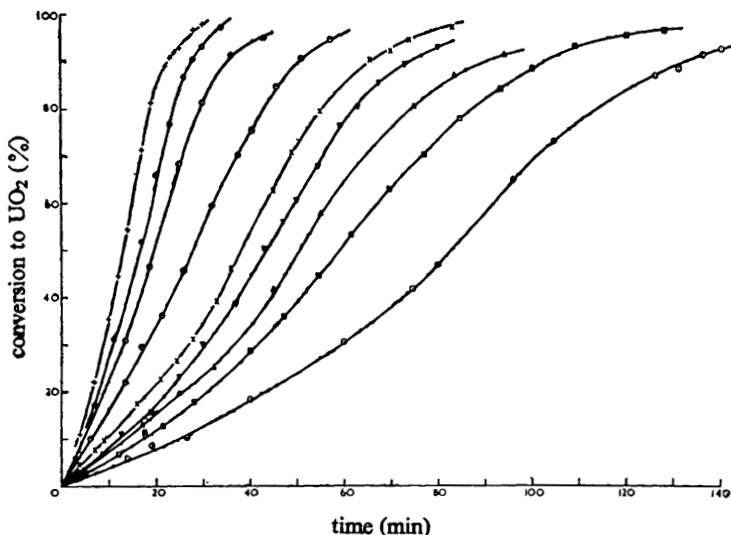


FIG. 1.—Hydrogen reduction of standard low-sulphate UO_3 .

○ 503°C ; □ 510°C ; △ 520°C ; ▽ 526°C ; × 529°C ; ● 548°C ; ⊙ 560°C ; ● 572°C ; + 592°C

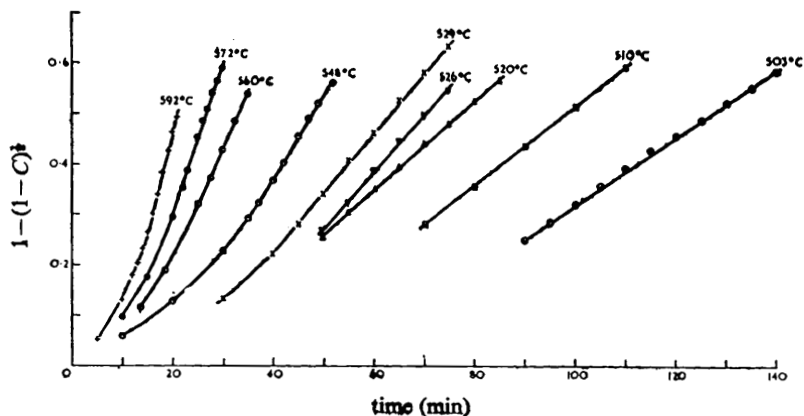


FIG. 2.—Reaction velocity plots for reduction of UO_3 .

areas are lower than the corresponding values for UO_2 prepared from sulphated UO_3 which exceed $2 \text{ m}^2/\text{g}$.⁶ Density values for the UO_2 samples show the particles to be highly porous (9 % by volume closed porosity and 29 % open porosity). This porosity is a consequence of the increase in crystallite density in going from UO_3 to UO_2 , coupled with the relatively small contraction in molar specific particle volume. Microscopic examination of the fully reduced UO_2 reveals that the core and shell structure is more pronounced than for the parent UO_3 . A soft, friable core is sur-

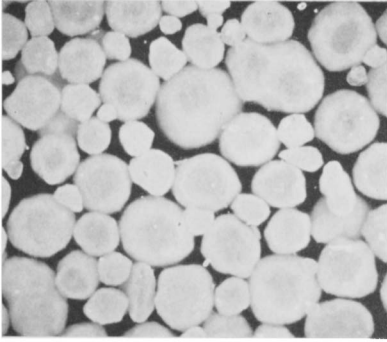


PLATE 1.—Particle cross-sections for a typical sample of fluidized-bed UO_3 ($\times 40$).

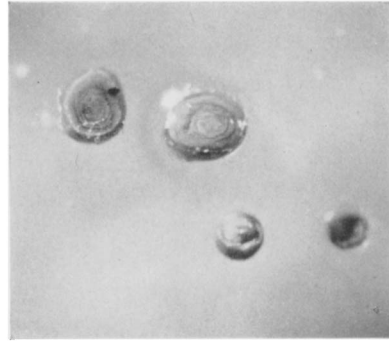


PLATE 2.—Illustrating "onion-ring" and "core and shell" type structures ($\times 40$).

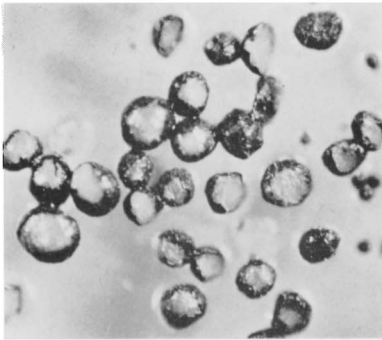


PLATE 3.—Partially reduced UO_3 ($\times 40$).

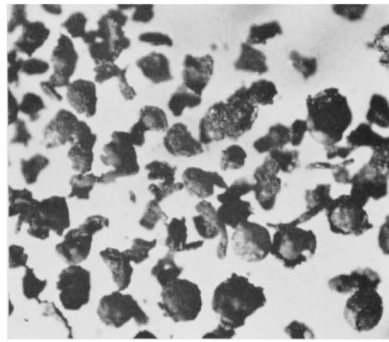


PLATE 4.— U_3O_8 prepared by oxidation of UO_2 ($\times 40$).

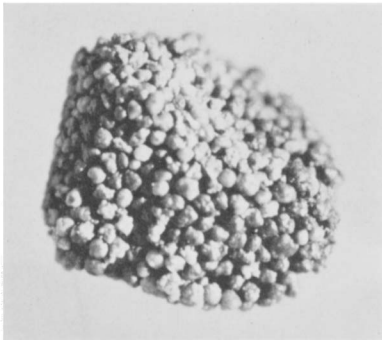


PLATE 5.— UF_4 produced by hydrofluorination at 650°C ($\times 10$).

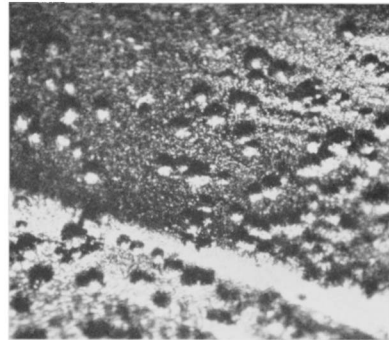


PLATE 6.—Surface of UO_2 single crystal after treatment with HF at 450°C ($\times 250$).

[To face page 1594

rounded by a hard, shiny shell, almost black in colour. The particles are reasonably robust, but do not possess the mechanical strength of UO_3 . On cracking open, the shell fractures and frequently breaks away in discrete pieces leaving the particle core exposed.

TABLE 1.—PHYSICAL PROPERTIES OF UO_3 , U_3O_8 , UO_2 (LOW SULPHATE SAMPLES) (80-120 mesh fraction)

material	preparation	surface area m^2/g	X-ray crystallite density g/cm^3	CCl_4 density g/cm^3	closed porosity (1)	mercury density g/cm^3	open porosity (2)	molar specific particle volume (3) cm^3
UO_3	fluid bed, low-sulphate UO_3	0.07	7.3-8.0	7.11	3-12 %	6.96	2 %	41.3 (4)
UO_2	UO_3 reduced by H_2 at 520°C	1.83	10.97	10.00	9 %	7.21	29 %	37.5
	UO_3 reduced by H_2 at 620°C	1.22						
U_3O_8	UO_3 decomposed at 650°C	0.09	8.39	6.76	20 %	6.69	1 %	42.0
	UO_3 decomposed at 750°C	0.08				6.40		43.8
	UO_3 decomposed at 890°C					6.37		44.0
UO_2 (via U_3O_8)	$\text{UO}_3 \rightarrow \text{U}_3\text{O}_8 \xrightarrow{\text{H}_2, 520^\circ} \text{UO}_2$	1.13	10.97					
	$\text{UO}_3 \xrightarrow{\text{H}_2, 720^\circ} \text{U}_3\text{O}_8 \xrightarrow{\text{H}_2, 520^\circ} \text{UO}_2$	0.63		9.63	12 %	6.87	29 %	39.3
	$\text{UO}_3 \xrightarrow{\text{H}_2, 720^\circ} \text{U}_3\text{O}_8 \xrightarrow{\text{H}_2, 520^\circ} \text{UO}_2$	} 0.63						
	sinter UO_2 in H_2 at 620°C							
U_3O_8	$\text{UO}_3 \xrightarrow{\text{H}_2, 750^\circ} \text{U}_3\text{O}_8 \xrightarrow{\text{H}_2, 520^\circ} \text{UO}_2 \xrightarrow{\text{air}} \text{U}_3\text{O}_8$	2.39						

Notes.—(1) closed porosity = $(1/\rho_{\text{CCl}_4} - 1/\rho_{\text{X-ray}})/\rho_{\text{CCl}_4}$; (2) open porosity = $(1/\rho_{\text{Hg}} - 1/\rho_{\text{CCl}_4})/\rho_{\text{Hg}}$; (3) molar specific particle volume = $\text{m.wt.}/\text{Hg density}$; (4) corrected for volatile content of UO_3 (0.44 %).

Tomlinson has demonstrated that the rate of reduction of UO_3 increases with its surface area,⁶ as might be expected for a reaction proceeding by a phase boundary mechanism. In order to determine whether the kinetics of reduction depend also

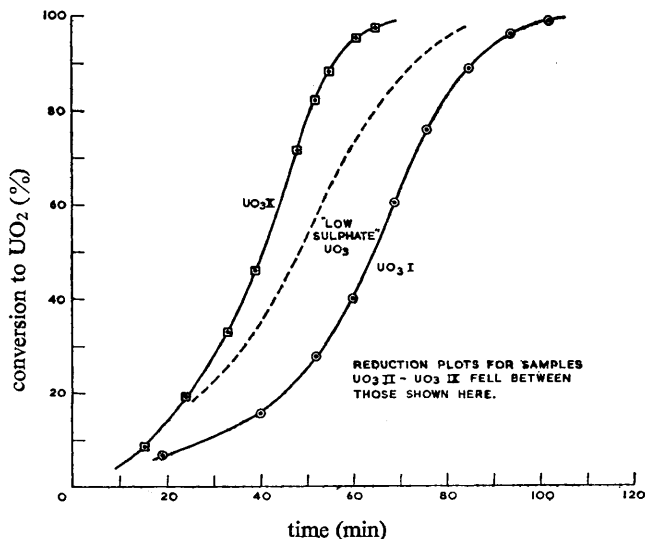


FIG. 3.—Hydrogen reduction of sulphated UO_3 samples at 520°C .

upon the *internal* particle texture, the ten separate preparations of sulphated UO_3 ($\text{UO}_3\text{I}-\text{UO}_3\text{X}$) were reduced in hydrogen at 520°C . Results for two of these preparations are shown in fig. 3, with a curve for low-sulphate UO_3 of similar size

fraction included for comparison. The plots for the remaining eight samples all fell between the two extreme curves shown and are omitted for clarity. These experiments show that the texture of the UO_3 particle does to some extent influence the rate of reduction. Examination of individual particles from a partly reduced sample showed an even wider variation in reduction rate from particle to particle; this tended to be averaged out in the aggregate samples.

REDUCTION OF UO_3 BY CARBON MONOXIDE

Fig. 4 shows kinetic curves for the reduction of UO_3X by carbon monoxide at 423-520°C. The curve for hydrogen reduction at 520°C is included, from which it is seen that reduction at a given rate in CO takes place at about 80°C lower than in

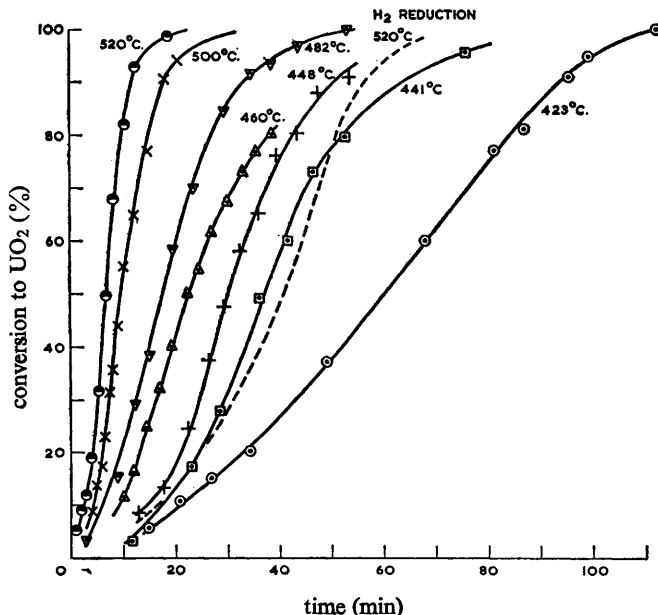


FIG. 4.—Carbon monoxide reduction of UO_3X .

hydrogen. For standard unsulphated UO_3 a temperature about 100° less was required with CO. The curves are again sigmoidal in shape, indicating that reduction of the particle shells is slower than the cores. Analyses of the kinetics using the Spencer-Topley equation gave straight line plots over the latter 40 % of the reaction from 440-520°C. The calculated activation energy was 31 ± 2 kcal/mole, a value close to that for hydrogen reduction. The activation energy for the first part of the reaction (20-60 % conversion) was estimated from the linear portion of the reduction curves at 26 ± 2 kcal/mole. Again, optical examination revealed that the reaction proceeded from the exterior of the particles inwards and X-ray study showed the presence of $\text{UO}_{2.6}$ as an intermediate phase.

DECOMPOSITION OF UO_3 TO U_3O_8

Decomposition of fluidized bed UO_3 to U_3O_8 first becomes significant at about 600°C. Measurements have been made of the decomposition kinetics of unsulphated oxide in flowing nitrogen from 623° to 700°C. The temperature was first taken up to 600°C and then raised as rapidly as possible in order to minimize decomposition

below the desired control temperature; even so, at the higher temperatures significant decomposition occurred before readings could be taken. The kinetic curves are presented in fig. 5.

Examination of partially decomposed samples showed that this reaction also proceeded by a phase-boundary mechanism, the particles exhibiting black outer shells (U_3O_8) with yellow centres (unconverted UO_3). This was equally true when decomposition was effected in a stream of oxygen rather than nitrogen. X-ray study showed no intermediate phases. Again the reaction rate varied from particle to particle; nevertheless the Spencer-Topley equation gave good linear plots over the

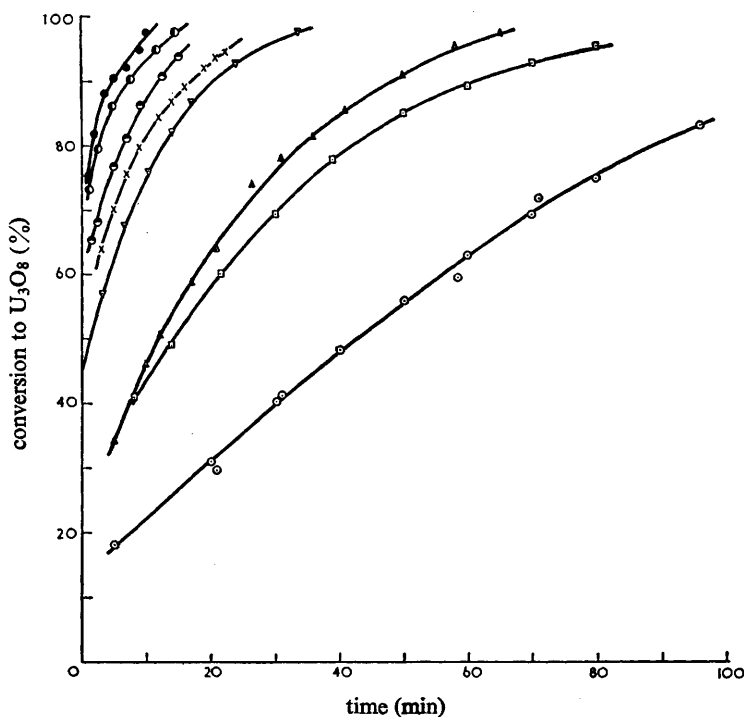


FIG. 5.—Decomposition of UO_3 to U_3O_8 in nitrogen.

○ 623°C; □ 636°C; △ 653°C; ▽ 668°C; × 680°C; ● 687°C; ⊙ 696°C; ● 700°C

major portion of the reaction, and from these an activation energy of 41 ± 2 kcal/mole was calculated. When decomposition was very rapid as, for example, when UO_3 was heated in a crucible over a burner, it was observed that some of the particles fractured into two. This process occurred with almost explosive force, causing the recoiling fragments to jump 1-2 cm above the surface of the bed. (For this reason a cover to the platinum bucket was necessary during thermogravimetric studies.) The incidence of fractured particles was low (<10 %) but rose to 30-50 % when rapid decomposition was carried out *in vacuo* at 650°C. Fracture occurs as a result of pressure build-up within the interior of the particle. It is unlikely that this pressure results from expansion of the core within the shell since the crystal density of U_3O_8 is greater than that of UO_3 . Rather, the internal pressure may be identified as the dissociation pressure of oxygen in equilibrium with UO_3 , within a non-porous shell of U_3O_8 . Surface area measurements show that the product U_3O_8 has a specific surface of ~ 0.08 m²/g, a value even lower than that of the parent UO_3 heated to

400° (0.15 m²/g). It follows that the U_3O_8 shell is non-porous, and also that sintering of U_3O_8 must occur at 650-700°C, in agreement with previous workers.² Further light is shed on the structure of the U_3O_8 particles by density determinations. The CCl_4 density of U_3O_8 prepared from 80-120 mesh UO_3 by heating at 680-700°C in air was 6.76 g/cm³ (table 1). This is significantly less than the X-ray crystallite density (8.39 g/cm³) and corresponds to a closed porosity of ~20%. This closed porosity was demonstrated directly by crushing the U_3O_8 and remeasuring the CCl_4 density. A value of 7.19 g/cm³ was measured. Since the closed porosity of UO_3 is <12% it is clear that an increase has occurred during the decomposition reaction. However, the U_3O_8 is known to possess little or no open porosity (low surface area) and so it seems that an expansion may have occurred in the overall particle size. That this is indeed the case was verified by direct mercury density determinations. Samples of U_3O_8 prepared at 650°C, 750°C and 890°C, by plunging UO_3 (80-120 mesh) into a preheated oven, were found to possess mercury densities of 6.69, 6.40 and 6.37 g/cm³ respectively. Computing the molar specific volumes and comparing with that of UO_3 , it is found that these densities correspond to average expansions of 1.7%, 6.1% and 6.5% in the volume of the particles.

The conclusion from these experiments is that when fluidized-bed UO_3 is heated to ~650°C, decomposition commences at the surface of the particles, whilst in the cores a dissociation pressure of oxygen in equilibrium with UO_3 builds up. If the temperature increases rapidly, the dissociation pressure becomes greater and causes the particles to expand by a few percent. For a minority of particles the yield point is exceeded and the particles fracture. Decomposition in vacuum leads to a greater pressure differential across the particle shells and a larger incidence of fracture. The expansion phenomenon preceding fracture is of some consequence in determining the reactivity of UO_2 prepared from U_3O_8 towards hydrofluorination.

REDUCTION OF U_3O_8 BY HYDROGEN

Two series of kinetic measurements were made. In the first series, a number of U_3O_8 samples were prepared from low-sulphate UO_3 by decomposition under varying conditions. The samples were then reduced to UO_2 at two standard temperatures (520° and 540°C), in order to determine whether the reduction rate was dependent upon the parameters of the UO_3 decomposition reaction. The results are presented in fig. 6 for seven different preparations of U_3O_8 , prepared either by heating UO_3 gradually to the desired temperature or by "plunging" into a preheated furnace. For comparison purposes the standard curve for reduction of UO_3 at 520° is included. The conclusions from these experiments are (i) the rate of reduction of U_3O_8 by hydrogen is essentially independent of the parameters of the decomposition reaction in which the oxide was prepared from UO_3 . (ii) At 520°C the rate of reduction of U_3O_8 is somewhat faster than that of the parent UO_3 . (iii) The sigmoidal nature of the UO_3 reduction curves has largely disappeared. The constant reduction rate for U_3O_8 samples prepared over a wide temperature range is at first sight surprising, having regard to the known sintering of U_3O_8 at these temperatures² and the observed variable expansion of the particles during their preparations from UO_3 . Presumably the low values for the surface area (~0.08 m²/g) and open porosity of the U_3O_8 lead to the reduction again following the decreasing-sphere mechanism, when the rate will not be greatly dependent upon the degree of sintering of the crystallites within the particle. Support for this mechanism is provided by X-ray studies of partially reduced samples, which show a higher ratio of $\text{UO}_2/\text{U}_3\text{O}_8$ in uncrushed samples than in crushed samples. No evidence for the $\text{UO}_{2.6}$ phase was found. The reaction interface is not observable directly as the product UO_2 has the same colour as U_3O_8 .

Further evidence is provided in Notz' observation² that there exists a linear relationship between mean particle diameter and hydrogen reduction time of U_3O_8 . The decreasing-sphere reaction mechanism does not, however, lead to linear reduction plots. A likely explanation of the approximately linear plots observed is that the increased reactivity of the porous particle core, as compared with the non-porous shell, almost balances the decreased rate due to the diminishing reaction interface, leading to a rate which is sensibly constant.

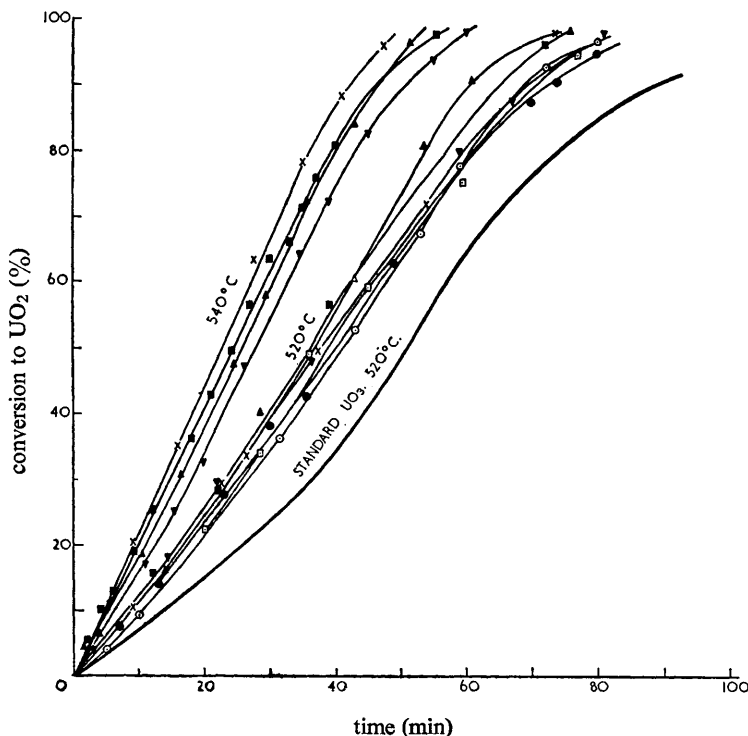


FIG. 6.—Hydrogen reduction of various U_3O_8 preparations at 520°C and 540°C.

○ decomposed gradually in a stream of N_2	623°C
□ decomposed gradually in a stream of N_2	687°C
● U_3O_8 I plunged into hot furnace	704°C
■ U_3O_8 II plunged into hot furnace	752°C
▲ U_3O_8 III plunged into hot furnace	792°C
▼ U_3O_8 IV plunged into hot furnace	840°C
× U_3O_8 V plunged into hot furnace	902°C

The surface area of UO_2 prepared from UO_3 via U_3O_8 is markedly dependent upon the sintering which occurs in the decomposition reaction but not upon that in the reduction reaction, which takes place at a lower temperature (table 1). This result is of interest in connection with hydrofluorination experiments. Density measurements revealed the porosity of the UO_2 to be comparable with that of UO_2 prepared by direct reduction of UO_3 .

In the second series of kinetic experiments, the reduction of a single sample of U_3O_8 was studied over a range of temperature in order to determine the activation energy of the reaction. The U_3O_8 sample employed was that prepared by rapid

decomposition of UO_3 at 752° by plunging into a preheated oven (air atmosphere). Rate measurements were made from 500° to 599° (fig. 7). The approximately linear reduction curves permitted direct measurement of the velocity constants. From their temperature coefficient the activation energy was determined as 31 ± 2 kcal/mole.

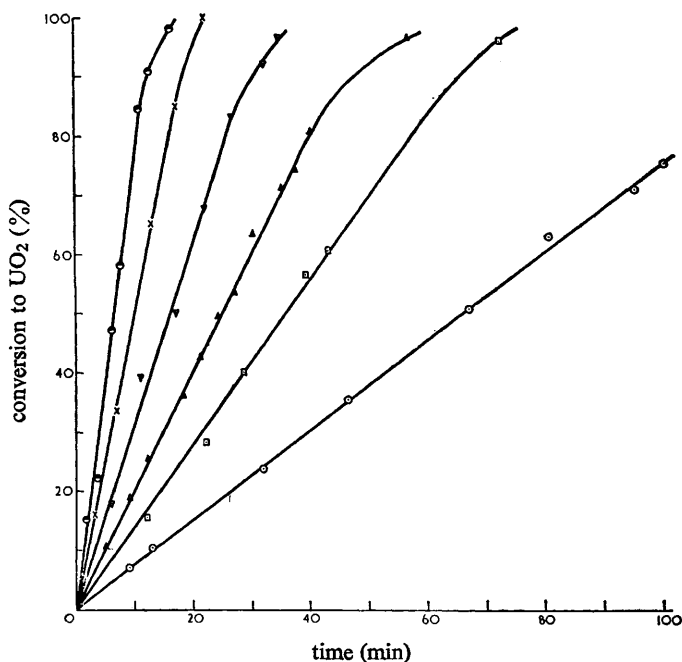


Fig. 7.—Hydrogen reduction of U_3O_8 as a function of temperature.
 ○ 500°C ; □ 520°C ; △ 540°C ; ▽ 559°C ; × 578°C ; ● 599°C

REOXIDATION OF UO_2

Rapid re-oxidation of UO_2 prepared from fluidized-bed UO_3 , by exposure to air or oxygen at 500 – 600°C , results in extensive disintegration of the physical structure of the particles, with fragmentation of the outer shell (plate 4). Under more gentle conditions of oxidation the particles hold together, but their surfaces exhibit extensive cracking. In this condition the particles possess little mechanical strength and readily crush. The oxidation is accompanied by an increase in surface area, for example from 0.6 m^2/g UO_2 to 2.4 m^2/g U_3O_8 . Since reduction of U_3O_8 to UO_2 also results in an area increase, the cyclic oxidation-reduction process provides a method of increasing the surface area of UO_2 , at the expense of particle break-up. The reduction is very rapid on account of the high surface area of the U_3O_8 ; in one experiment hydrogen reduction was complete in 5 min at 520°C (cf. fig. 1).

The oxidation of UO_2 involves an increase in crystallite volume (crystal density $\text{UO}_2 = 10.97$, $\text{U}_3\text{O}_8 = 8.39$ g/cm^3). The fact that surface area is developed in this reaction indicates that oxidation must involve fragmentation of the individual UO_2 crystallites within the particle. It is this phenomenon which explains the disintegration of the particle.

HYDROFLUORINATION OF UO_2

The kinetics of hydrofluorination of UO_2 prepared by direct reduction of fluidized-bed UO_3 were studied in detail by Tomlinson *et al.*⁷ The reaction is initially very

rapid at 450°C, but soon falls off to a diffusion-controlled reaction of activation energy 10 kcal/mole as a product layer of UF_4 is formed. For UO_2 of surface area less than $2 \text{ m}^2/\text{g}$, the reaction did not proceed to completion. The investigation is now extended to include a comparison of the relative reactivities of UO_2 samples prepared under different conditions.

Fig. 8 illustrates the hydrofluorination kinetics at 450°C for UO_2 prepared from unsulphated UO_3 by direct hydrogen reduction (upper four curves) and via U_3O_8 (lower curves). In no experiment does the conversion in one hour exceed 60%.

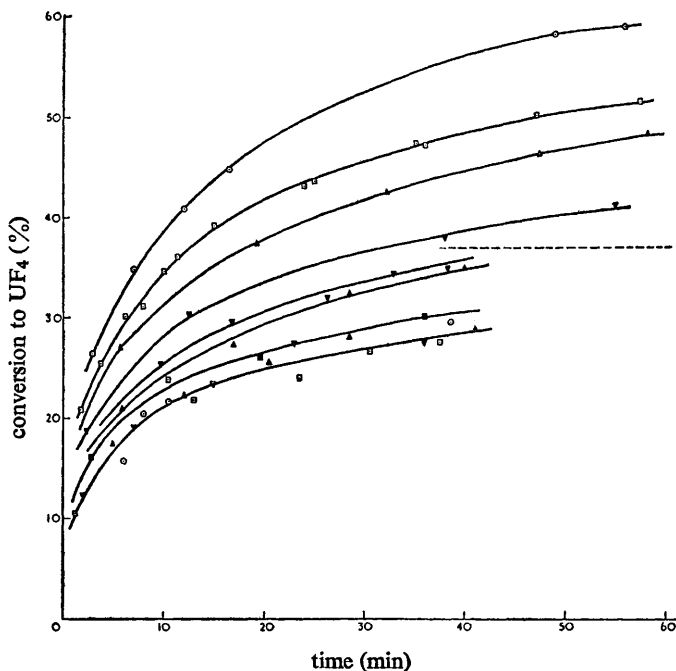


FIG. 8.—Hydrofluorination of UO_2 at 450°C.

	UO_2 ex- UO_3 redn.	UO_2 ex- U_3O_8 decomp.	UO_2 ex- U_3O_8 redn.	
upper curves	○ 500°C	○ 752°C	○ 500°C	} lower curves
	□ 520°C	□ 752°C	□ 520°C	
	△ 560°C	△ 752°C	△ 540°C	
	▽ 595°C	▽ 752°C	▽ 578°C	
	■ 792°C	■ 520°C		
	▲ 840°C	▲ 520°C		
	▼ 903°C	▼ 520°C		

For direct reduction of UO_3 , the extent of hydrofluorination decreases with increasing reduction temperature. This correlates with a decrease in UO_2 surface area (table 1). Two series of experiments were performed on the hydrofluorination of UO_2 prepared from U_3O_8 . In the first, a large sample of U_3O_8 was prepared from UO_3 by a single decomposition in air at 752°C; fractions of this oxide were then reduced at various temperatures from 500-578°C and the rate of hydrofluorination at 450°C measured as a function of the reduction temperature. In the second series, samples of U_3O_8 prepared by UO_3 decomposition in air at temperatures from 752-902°C were reduced at 520°C and the hydrofluorination rate at 450°C measured as a function of the decomposition temperature. The results showed: (i) the rate of hydrofluorination of

UO_2 prepared from U_3O_8 was always less than that of UO_2 prepared directly from UO_3 , (ii) the rate was independent of the reduction temperature (in marked contrast to the results for UO_2 prepared by UO_3 reduction), (iii) the hydrofluorination of UO_2 ex- U_3O_8 was favoured by increasing temperatures of decomposition of UO_3 to U_3O_8 . The significance of these results will be discussed later.

Hydrofluorination of UO_2 derived from sulphated UO_3 proceeded to completion far more readily. Fig. 9 illustrates the kinetics of hydrofluorination, at temperatures from 250°C to 650°C , of UO_2 prepared from UO_3X by reduction at 520°C . At 450 - 550°C reaction proceeds to virtual completion in an hour. All ten samples of sulphated UO_3 ($\text{UO}_3\text{I-X}$) were reduced at 520°C and hydrofluorinated at 450°C .

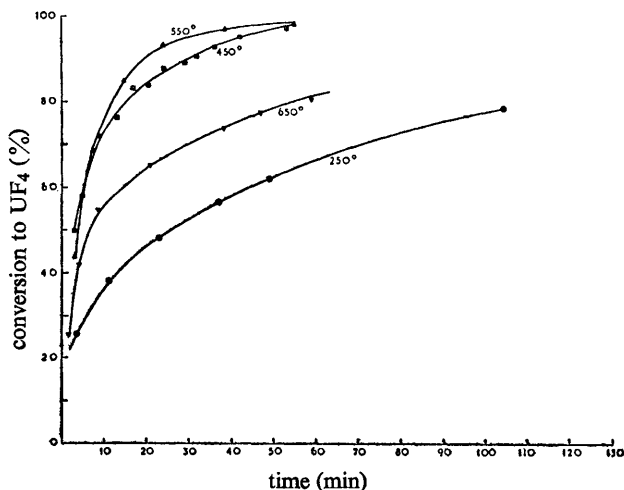


FIG. 9.—Hydrofluorination at various temperatures of UO_2 prepared from sulphated UO_3 by hydrogen reduction at 520°C .

There was found to be no significant dependence of hydrofluorination rate upon particle texture of sulphated UO_2 ; all the kinetic curves lay within 2-3 % of the 450°C curve shown. At temperatures above 550°C a "thermal deactivation" phenomenon arose, the rate of reaction at 650°C being markedly less than at 550°C . This result is ascribed to sintering of the product layer of UF_4 first formed on the exteriors of the UO_2 crystallites; such sintering may be expected having regard to the low melting point of UF_4 (960°C). A similar deactivation effect was found also for UO_2 derived from unsulphated UO_3 . The blackened points on the 450° curve refer to a sample of reduced UO_2 heated to 650° in H_2 before hydrofluorination at 450°C . The absence of deactivation confirms that this phenomenon is associated with the UF_4 rather than the UO_2 .

Microscopic examination of samples of partially hydrofluorinated UO_2 revealed several points of interest. As noted previously,⁷ the particles remain black throughout until the reaction is well advanced; green UF_4 becomes apparent in the interiors of the particles at ~ 80 % conversion for the sulphated oxide but at a rather lower conversion (40-50 %) for the unsulphated oxide. For reaction at 450°C , the exteriors of the particles remain black even at ~ 100 % conversion, although the centres are mostly green. On continuing to interact with HF for prolonged periods (2-3 h) nuclei of green UF_4 become visible on the surface and spread over the particle until the exterior is entirely green; no weight change was detectable during this period.

The completely green UF_4 particles still possess the core and shell structure characteristic of fluidized-bed UO_3 . Individual particles show variations from this general behaviour, as discussed by Tomlinson.⁷ X-ray examination of uncrushed particles of UF_4 with black shells gave only the UF_4 pattern. The appearance of UF_4 prepared at 650°C differed from that formed at 450°C . In general, the particles were shiny rather than dull, while in some instances they were fused together into a cluster (plate 5). Both of these observations are manifestations of the sintering of UF_4 at 650°C .

Since the reactivity of unsulphated UO_2 increases with decreasing reduction temperature in hydrogen, it might be expected that reduction with carbon monoxide would give rise to a more reactive UO_2 . This was confirmed experimentally. Unsulphated UO_3 was reduced by CO at 390°C and then hydrofluorinated at 450°C ; the UO_2 was found to be 50 % converted to UF_4 in 5 min and 75 % in 20 min (cf. fig. 8 for hydrogen reduction). This result suggests that it is the *temperature* of reduction rather than the *rate* which determines the surface area of the UO_2 and thus its reactivity during hydrofluorination. Experiments with sulphated UO_2 showed the expected high reactivity towards hydrofluorination; for example, after CO reduction at 450°C hydrofluorination at the same temperature was complete in 40 min. Optical examination of UF_4 prepared in these latter runs showed the surfaces to be green after only one hour at 450°C and the particles exhibited a tendency to stick together. Both these effects may relate to the higher reactivity of UO_2 prepared by CO reduction. Attempted hydrofluorination at 650°C again led to marked thermal deactivation.

Other experiments included the reaction of HF with UO_2 prepared in the following ways: (i) low-sulphate $\text{UO}_3 \xrightarrow{\text{H}_2} \text{UO}_2 \xrightarrow{\text{air}} \text{U}_3\text{O}_8 \xrightarrow{\text{H}_2} \text{UO}_2$ and (ii) high-sulphate $\text{UO}_3 \xrightarrow{\text{H}_2} \text{UO}_2 \xrightarrow{\text{HF}} \text{UF}_4 \xrightarrow{\text{H}_2\text{O}} \text{UO}_2$. The hydrofluorination of the product from route (i) was 92 % complete in 10 min at 450°C . In route (ii) the UF_4 was hydrolyzed to UO_2 in a stream of wet nitrogen at 450°C ; subsequent hydrofluorination was complete in 7 min at 450°C . It is concluded that the porous expanded oxides formed in an oxidation-reduction cycle or on hydrolysis of UF_4 are highly reactive.

SINGLE CRYSTAL STUDIES

Some experiments were carried out on the hydrofluorination of single crystals of UO_2 prepared by electrolysis. Fig. 10 shows the conversion curve as a function of temperature and crystal size. Large single crystals hydrofluorinate very slowly even at 650°C ; at 500°C the conversion attained in 3 h was only 10 %. Smaller crystals hydrofluorinated more readily, but the maximum conversion reached was 35 % for -300 mesh material at 500°C . The one result obtained by Tomlinson⁷ (for -300 mesh UO_2 at 450°C) fits well with our data. From the known surface area of single crystals, the thickness of the UF_4 product layer may be computed; after 60 min this layer is ~ 3.5 microns thick at 500°C and ~ 2.5 microns at 450°C . Photomicrographic examination of the crystal after relatively slight hydrofluorination (3 % conversion at 450°C) revealed the existence of small eruptions or blisters on the surface; these were formed during the reaction (plate 6).

DISCUSSION

The reduction of fluidized-bed UO_3 to UO_2 has been shown to proceed by an interfacial reaction and to involve two separate steps, with $\text{UO}_{2.6}$ as the intermediate phase. The explanation of an interface reaction is to be found in the non-porous

nature of the shells of the UO_3 particles; reaction must necessarily start at the exterior of the particle and proceed inwards as porosity is developed. The porosity of the product UO_2 provides ready access for gas to and from the reaction interface. Hence the reaction is not diffusion controlled and the measured activation energy refers to a chemical step at the interface. Morrow, Graves and Tomlinson⁶ have discussed the reaction mechanism in detail and conclude that the rate-determining step is probably the adsorption of hydrogen on the UO_3 surface. While this may well be correct, it should be noted that the situation is complicated not only by the

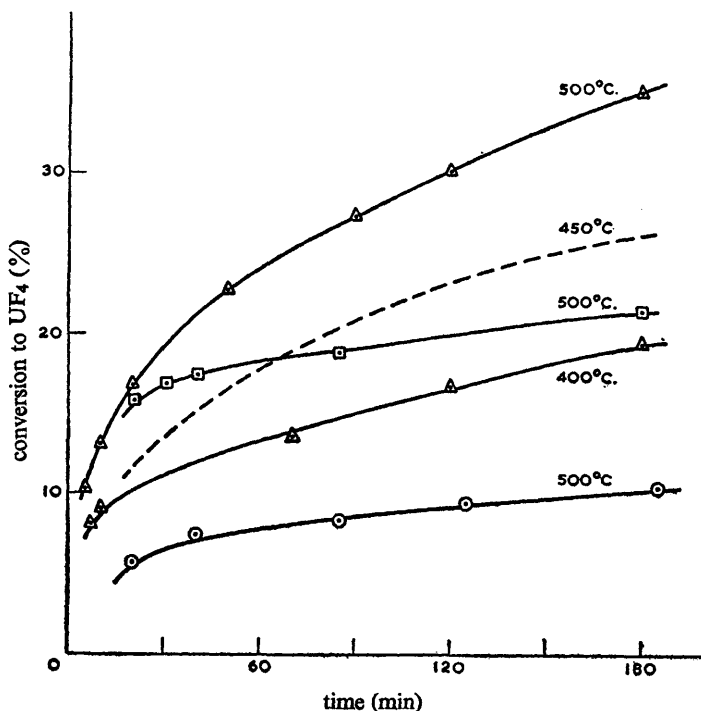


FIG. 10.—Hydrofluorination of UO_2 single crystals.

\circ +40 mesh crystals; \square -120+180 mesh; Δ -300 mesh;
- - - -300 mesh, result taken from ref. (7).

occurrence of two simultaneous reactions and by the higher intrinsic reactivity of UO_3 in the particle centres to that in the outer shells, but also by a variation in reactivity from preparation to preparation and from particle to particle. It is evident that the reduction of UO_3 is a highly texture-sensitive reaction. Nevertheless, the reasonable agreement between the activation energy measured in the present investigation (28 ± 2 kcal/mole) and in previous studies using UO_3 of widely differing texture^{2-4,6} inspires confidence that a uniform reaction mechanism and rate-determining step is involved. One may envisage chemisorption of hydrogen on the outermost UO_3 crystallites, followed by surface reaction with the formation of oxide ion vacancies and desorption of water. When the surface concentration of anion vacancies exceeds a critical value, nucleation of the lower oxide ($\text{UO}_{2.6}$ phase) will occur, followed by growth of this new phase into the UO_3 crystallite. Further reaction at the surface of the $\text{UO}_{2.6}$ phase will lead to a depletion of the oxygen content until an unstable state is again reached and UO_2 nucleates and grows. Superimposed

upon this reaction mechanism for each UO_3 crystallite will be the observed macroscopic propagation of the reaction interface into the interior of the particle. Using carbon monoxide as the reducing agent, the activation energy is not far different from that for hydrogen, but the reaction may be effected at a significantly lower temperature. The relative ease of reduction may be understood either in terms of the lower activation energy for adsorption of CO (no molecular dissociation being involved) or in terms of the known ease of desorption of CO_2 from oxides compared with water.

The thermal decomposition of all six forms of UO_3 has been studied by Hoekstra and Siegel,¹ who also find no intermediate phase between UO_3 and U_3O_8 , except for amorphous UO_3 which decomposes via the $\text{UO}_{2.9}$ phase. The only reported activation energy for UO_3 decomposition is that of Vlasov and Lebedev¹¹ for amorphous UO_3 , who find a value of 37 kcal/mole. This compares with the present result of 41 ± 2 kcal/mole for γUO_3 .

The reduction of U_3O_8 to UO_2 has been reported briefly in the project literature;² the activation energy mentioned (34 kcal/mole) agrees reasonably with the present value (31 ± 2 kcal/mole). The fact that the activation energy for U_3O_8 reduction is close to that for UO_3 reduction suggests that a similar rate determining step may be involved.

HYDROFLUORINATION

The hydrofluorination of UO_2 to UF_4 is a reversible process and in the temperature range of interest (400-600°C) the back reaction $\text{UF}_4 + 2\text{H}_2\text{O} \rightarrow \text{UO}_2 + 4\text{HF}$ is significant, e.g., at 500°C the equilibrium constant has a value $\log k_p = -2.916$.¹² For this reason, gas-diffusion problems in the pores of a UO_2 particle are difficult to avoid, particularly in the early stages of the reaction where the intrinsic rate is very high. Conversion of UO_2 (crystal density 10.97 g/cm³) to UF_4 (crystal density 6.70 g/cm³) is associated with a large volume expansion. As reaction proceeds many of the pores in the UO_2 particle become blocked or sealed off by UF_4 , resulting in a decrease in surface area,⁷ and further reaction is limited by the rate of diffusion of HF through the product layer. It is this latter process which has an activation energy of 10 kcal/mole. Support for this model is provided by the single crystal studies. If a product layer of UF_4 of 2.5 microns thickness formed around every UO_2 crystallite, then the reaction would proceed to completion for all polycrystalline UO_2 samples of surface area greater than ~ 0.1 m²/g. Since, in practice, a surface area of ~ 2 m²/g is necessary to ensure rapid and complete reaction it follows that much of the UO_2 surface area is not available for hydrofluorination, as it is present in pores which are sealed off during the early stages of reaction.

A question of interest is why the UF_4 product layer may form to a depth of several microns before reaction is significantly impeded. It is suggested that after the initial formation of a thin coherent UF_4 layer, further reaction is possible by diffusion of HF through this layer to the reaction interface. Localized regions will then exist where the gaseous reaction product (steam) builds up to a high pressure internally. The explosive release of this steam through the UF_4 layer gives rise to blisters (plate 6) and these may serve as a means of access for further HF. In this way the product layer may build up to a depth of several microns before reaction is finally impeded. A similar phenomenon has been observed during the reduction of copper oxide by hydrogen.¹³

The mechanism whereby sulphate additive facilitates hydrofluorination is of some interest. A specifically chemical role for the sulphur is ruled out by the fact that it is largely eliminated as H_2S during reduction.

The suggestion has been made that the additive serves to retard denitration during the decomposition of uranyl nitrate. The subsequent escape of nitrogen oxides from the interior of a particle then gives rise to a more porous, reactive UO_3 ,^{2,6} which, in turn, yields a more reactive form of UO_2 . Certainly, the surface area of fluidized-bed UO_3 increases with sulphate content, suggesting that the sulphate additive fulfils its function during the decomposition reaction rather than during reduction. Moreover, the surface area and reactivity of the UO_2 is found to increase regularly with the UO_3 surface area. From a consideration of the above model of hydrofluorination, it is not obvious that a high surface area UO_2 will invariably be reactive, particularly if much of this surface area is located in fine pores which are sealed off early in the reaction. Indeed, experiments with UO_2 prepared from UO_3 hydrates (to be published) show that a high surface area ($> 2 \text{ m}^2/\text{g}$) is a necessary but not always sufficient criterion of reactivity towards hydrofluorination. It is therefore of interest to determine whether the sulphated and unsulphated oxides differ in properties other than surface area. One report states that sulphated UO_3 is less crystalline than unsulphated UO_3 ,² but our X-ray diffraction patterns do not support this finding. We have therefore measured the carbon tetrachloride and mercury densities for sulphated and unsulphated UO_3 and UO_2 and also compared the pore size distributions for the two UO_2 's determined from nitrogen adsorption isotherms and by mercury porosimetry. The results, in brief, were as follows; (i) sulphated UO_3 is rather more porous than unsulphated UO_3 ; molar specific volume = 44.7 cm^3 ; (ii) there is little difference in the total porosity of the dioxides (40 % for sulphated UO_2 compared with 38 % for unsulphated), although the ratio of open porosity/closed porosity is rather higher in the sulphated sample; (iii) the majority of the pores for both types of UO_2 lie in the size range 0.3-1.0 microns diameter with comparatively few pores of diameter < 0.3 microns. These various experiments revealed no major differences in porosity or in pore-size distribution which might reasonably account for the striking difference in UO_2 reactivity and it is concluded that for UO_2 prepared by direct reduction of fluidized-bed UO_3 the reactivity towards hydrofluorination is a function principally of its surface area. Since, for a given reduction temperature, the UO_2 surface area is primarily a function of sulphate content in the UO_3 , this further explains why no difference in reactivity was found between the ten samples of similar sulphate content.

The reactivity of UO_2 prepared via the U_3O_8 intermediary is more complex. It was shown that the rate of hydrofluorination is less than that of UO_2 prepared directly and is independent of the reduction temperature. These two observations may be understood in terms of the lower surface area of UO_2 prepared via U_3O_8 (table 1). This low surface area is a result of the sintering which takes place at the temperature of decomposition of UO_3 . Consequently the reactivity of the UO_2 towards hydrofluorination is determined by the course of the $\text{UO}_3 \rightarrow \text{U}_3\text{O}_8$ decomposition rather than by the subsequent reduction to UO_2 . Nevertheless, it is at first sight surprising that the hydrofluorination reaction rate *increases* slightly with increase of UO_3 decomposition temperature (i.e., of U_3O_8 sintering temperature). The explanation for this may lie in the observed swelling of the particles during decomposition. This expansion will increase the voidage within the particle and so will facilitate the hydrofluorination reaction which requires a 90 % increase in crystal volume. An interesting feature of this result is that the structure of the U_3O_8 particle, as determined in the decomposition reaction, influences the rate of UO_2 hydrofluorination without showing any influence on the rate of the intervening reduction reaction (fig. 6). It is concluded that the rate of a solid/gas reaction may, in certain circumstances, be conditioned by the structure of the solid as determined in a pen-

ultimate reaction, without this structural factor playing any role in the intervening reaction.

Finally, reference may be made to the black form of UF_4 which occurs in these experiments. Varwig and Kennelly¹⁴ also observed green particles with black shells and concluded that hydrofluorination proceeded "from the inside out", the particle shells converting last to UF_4 . This conclusion has now been shown to be erroneous. The exact nature of black UF_4 remains uncertain. Higher fluorides of uranium are known which are black in colour (U_2F_9 , U_4F_{17}). To ensure that these were not formed, through the presence of adventitious oxidizing impurities, an experiment was carried out in which hydrogen was mixed with the hydrogen fluoride gas stream to ensure reducing conditions. The UF_4 formed possessed the usual black outer layer to the particles, confirming that this black material is not associated with the presence of uranium ions in higher valence states. Rather, it seems likely that black UF_4 is a slightly distorted form of the usual structure arising either from the presence of residual oxide or hydroxide ions in the UF_4 lattice, or from pressure effects exerted during hydrofluorination. The presence of oxide ions in the UF_4 lattice to form a phase UO_xF_{4-2x} is not easy to distinguish analytically from residual unreacted UO_2 , although the similar diameters of O^{2-} and F^- ions makes this substitution plausible. Alternatively, evidence for the influence of pressure has been presented by Barnes and Murray¹⁵ who find that sintering and hot pressing of UF_4 leads to a black form of the fluoride. On this model the occurrence and location of regions of black UF_4 in a fluidized-bed particle will depend on the stresses set up during hydrofluorination as a result of crystal expansion. These stresses will be related to the internal texture and porosity of the UO_2 particle.

The authors are indebted to Dr. L. E. J. Roberts and Dr. L. Tomlinson for many helpful discussions. The experimental assistance of Mr. R. Junkison is also gratefully acknowledged.

¹ Hoekstra and Siegel, *J. Inorg. Nucl. Chem.*, 1961, **18**, 154.

² Harrington and Rühle, (ed.) *Uranium Production Technology* (van Nostrand, 1959).

³ Demarco and Mendel, *J. Physic. Chem.*, 1960, **64**, 132.

⁴ Notz and Mendel, *J. Inorg. Nucl. Chem.*, 1960, **14**, 55.

⁵ Jonke, Petkus, Loeding and Lawroski, *Nucl. Sci. Eng.*, 1957, **2**, 303.

⁶ Morrow, Graves and Tomlinson, *Trans. Faraday Soc.*, 1961, **57**, 1400.

⁷ Tomlinson, Morrow and Graves, *Trans. Faraday Soc.*, 1961, **57**, 1008.

⁸ Dell and Wheeler, *A.E.R.E. Report R-3424* (1960). (The Use of Helical Springs in Physico-Chemical Research; H.M.S.O.).

⁹ Robins, *J. Nucl. Materials*, 1961, **3**, 294.

¹⁰ Spencer and Topley, *J. Chem. Soc.*, 1929, 2633.

¹¹ Vlasov and Lebedev, *Isv. vyssh. uch. zav. Chernaya Metallurgia*, 1960, no. 7, p. 5.

¹² Domange and Wohlhuter, *Compt. Rend.*, 1949, **228**, 1591.

¹³ Garner, Gray and Stone, *Proc. Roy. Soc. A*, 1949, **197**, 294.

¹⁴ Varwig and Kennelly, *U.S.A.E.C. Technical Report MCW 1430* (1959).

¹⁵ Barnes and Murray, *J. Amer. Ceramic Soc.*, 1958, **41**, 246.